Anal. Bioanal. Electrochem., Vol. 10, No. 1, 2018, 33-51

Analytical & Bioanalytical Electrochemistry

2018 by CEE
www.abechem.com

Full Paper

Experimental and Quantum Chemical Analysis of New Pyrimidothiazine Derivative as Corrosion Inhibitor for Mild Steel in 1.0 M Hydrochloric Acid Solution

Mohamed Larouj,[1, 2] Hassane Lgaz,[1, 2] Rachid Salghi,[2,*] Houda Serrar,[3] Said Boukhris[3] and Shehdeh Jodeh[4]

[1]*Laboratory separation processes, Faculty of Science, University Ibn Tofail PO Box 242, Kenitra, Morocco*

[2]*Laboratory of Environmental Engineering and Biotechnology, ENSA, University Ibn Zohr, PO Box 1136, 80000 Agadir, Morocco*

[3]*Laboratory of Organic Synthesis, Organometallic and theoretical, Faculty of Sciences, University Ibn Tofail, Kenitra, Morocco*

[4]*Department of Chemistry, An-Najah National University, P. O. Box 7, Nablus, Palestine*

*Corresponding Author, Tel.: +212528232007; Fax: +212528228313

E-Mail: r.salghi@uiz.ac.ma

Received: 14 June 2017 / Received in revised form: 26 September 2017 / Accepted: 23 November 2017 / Published online: 31 January 2018

Abstract- The corrosion inhibition efficiency of pyrimidothiazine compound, namely: 8-ethyl-3-hydroxy-4,6-dioxo-2-(p-tolyl)-4,6-dihydropyrimido [2,1-b][1,3] thiazine-7carbonitrile (EHDPTC), was evaluated in the system steel/1 M HCl. This compound is investigated experimentally using weight loss, potentiodynamic polarization curves and electrochemical impedance spectroscopy. The results showed that the inhibition mechanism involves blockage of the steel surface by the inhibitor molecules by a Langmuir-type adsorption process and that the structure of molecule plays an important role in the inhibition efficiency of the synthesized inhibitor. The thermodynamic parameters of activation and adsorption have been calculated and discussed in detail. Furthermore, the quantum chemical parameters have been calculated and discussed in view of the results earlier reported.

Keywords - Corrosion inhibition, Mild Steel, HCl, pyrimidothiazine, DFT

1. INTRODUCTION

Corrosion is a major problem in several industries. It causes enormous wastage of metallic materials. Mild steel is most important of engineering material particular for structural, instrumental, industrial and automobile applications due to its low cost and excellent mechanical properties. However, it is severely attacked in acid solutions in various industries during pickling cleaning of industrial equipment of oil well and other processes. Inhibited acid solutions are commonly used to reduce the corrosive attack of acid on metals. The use of inhibitor is the most important method for protecting metals from corrosion, and many scientists are conducting research on this topic. New inhibitors are discovered every day. In principle, inhibitors prevent the corrosion of metals by interacting with the metal surface via adsorption through the donor atoms, π orbitals, electron density and the electronic structure of the molecule [1–4].

Theoretical calculations have been used recently to explain the mechanism of corrosion inhibition, which proved to be a very powerful tool in this direction [5–7]. The geometry of inhibitor molecule in its ground state, nature of its molecular orbitals, HOMO and LUMO are directly involved in the corrosion inhibition activity.

The aim of this work is to study the inhibition effect of pyrimidothiazine derivative on the corrosion of mild steel at different concentrations and different temperatures in hydrochloric acid (HCl) solution. Electrochemical investigations, potentiodynamic polarization measurements, electrochemical impedance spectroscopy (EIS) weight loss, were employed for the exploration of inhibition efficiency of this organic compound.

2. MATERIALS AND METHODS

2.1. Materials and test solution

The steel used in this study is a carbon steel had the following composition (atom%):0.370% C, 0.230% Si, 0.680% Mn, 0.016% S, 0.077% Cr, 0.011% Ti, 0.059% Ni, 0.009% Co, 0.160% Cu and the remainder iron (Fe).The metal specimens used in weight loss studies have a rectangular form (length=1.6 cm, width=1.6 cm, thickness=0.07 cm). For electrochemical studies, same type of coupons was used but only 1 cm^2 area was exposed during each measurement. Before measurements, the samples were polished using different grades of emery papers SiC (120, 600 and 1200); and then subjected to the action of a buffing machine attached with a cotton wheel and a fiber wheel having buffing soap to ensure mirror bright finish, degreased by washing with ethanol, acetone and finally washed with distilled water.

The aggressive solutions of 1.0 M HCl were prepared by dilution of analytical grade 37% HCl with distilled water. The 8-ethyl-3-hydroxy-4,6-dioxo-2-(p-tolyl)-4,6-dihydropyrimido[2,1-b][1,3]thiazine-7carbonitrile used in the present study was prepared

according to previously published paper [8], the concentration range of used compound was 1×10^{-4} M to 5×10^{-3} M.

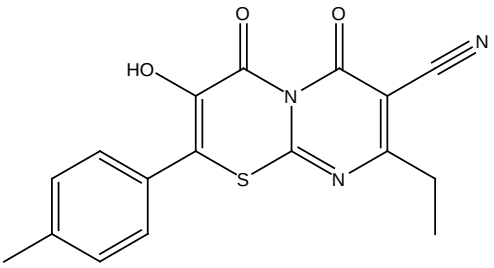

Fig. 1. Molecular structure of 8-ethyl-3-hydroxy-4,6-dioxo-2-(p-tolyl)-4,6-dihydropyrimido[2,1-b][1,3]thiazine-7carbonitrile

2.2. Weight loss measurements

Carbon steel specimens were accurately weighed and then immersed in 1.0 M HCl solutions without and with inhibitor for 6h at 303 K. After that, the specimens were withdrawn and carefully cleaned by distilled water and acetone, and then dried and weighed. Triplicate experiments were performed in each case and the mean value of the weight loss was calculated.

2.3. Electrochemical tests

Electrochemical tests were carried out in a conventional three electrode cell with platinum counter electrode, saturated calomel electrode as the reference electrode and the carbon steel with the surface area of 1 cm^2 as the working electrode. Electrochemical experiments were conducted using impedance equipment (Tacussel Radiometer PGZ 100) and controlled with Tacussel corrosion analysis software model VoltaMaster 4.

Before electrochemical tests, the working electrode was immersed in test solution at open circuit potential (OCP) for 30 min to attain a stable state. In order to minimize ohmic contribution, the tip of lugging capillary was kept close to working electrode. The potential of potentiodynamic polarization curves started from potential -800 mV to -300 mV *vs*. SCE with a scan rate of 1 mV s^{-1}. Electrochemical impedance spectroscopic studies were carried out at OCP in the frequency range of 10 mHz -100 kHz, with 10 points per decade, at the rest potential, after 30 min of acid immersion, by applying 10 mV peak to peak voltage excitation. Nyquist plots were made from these experiments. The best semicircle can be fit through the data points in the Nyquist plot using a non-linear least square fit so as to give the intersections with the x-axis.

2.5. Theoretical calculations

All calculations were performed using the GAUSSIAN 09 program package [9] with the aid of the GaussView visualization program[10]. The ground state geometry of EHDPTC was fully optimized using the hybrid B3LYP functional methods[11,12] in combination with the 6-31G (d, p) basis set.

The following quantum chemical parameters were calculated from the obtained optimized structure: The highest occupied molecular orbital (E_{HOMO}) and the lowest unoccupied molecular orbital (E_{LUMO}), the energy difference (ΔE) between E_{HOMO} and E_{LUMO}, dipole moment (μ), electron affinity (A), ionization potential (I) and the fraction of electrons transferred (ΔN).

According to Koopman's theorem [13] the ionization potential (I) and electron affinity (A) of the inhibitor are calculated using the following equations.

$$I = -E_{HOMO} \quad (1)$$

$$A = -E_{LUMO} \quad (2)$$

Thus, the values of the electronegativity (χ) and the chemical hardness (η) according to Pearson, operational and approximate definitions can be evaluated using the following relations[14]:

$$\chi = \frac{I+A}{2} \quad (3)$$

$$\eta = \frac{I-A}{2} \quad (4)$$

Chemical softness (σ) is the measure of the capacity of an atom or group of atoms to receive electrons[15], it is estimated by using the equation:

$$\sigma = \frac{1}{\eta} \quad (5)$$

The number of transferred electrons (ΔN) was also calculated depending on the quantum chemical method[16–18] by using the equation:

$$\Delta N = \frac{\phi - \chi_{inh}}{2(\eta_{Fe} + \eta_{inh})} \quad (6)$$

The obtained DFT derived ϕ values for Fe (1 0 0), Fe (1 1 0) and Fe (1 1 1) surfaces are 3.91, 4.82 and 3.88 eV, respectively [19,20]. In this study, we use only Fe (1 1 0) surface due to its higher stabilization energy and packed surface.

The local reactivity of inhibitor molecules were obtained by condensed Fukui functions [21]. Finite difference approximations have been used to get Fukui functions in favor of nucleophilic and electrophilic attacks as [22]:

$$f_k^+ = q_k(N+1) - q_k(N) \quad (7)$$

$$f_k^- = q_k(N) - q_k(N-1) \quad (8)$$

Here, gross charge of the atom *k* is denoted by q_k. The q_k $(N + 1)$, q_k (N) and q_k $(N - 1)$ are the charges of the anionic, neutral and cationic species, respectively.

3. RESULTS AND DISCUSSION

3.1. Weight loss measurements

The WL tests were performed in 1.0 M HCl at 303 K with different concentrations of the EHDPTC. The *IE* % and W_{corr} values obtained from the *WL* measurements of the carbon steel for various concentrations of the EHDPTC in studied medium at 303 K after 6 h of immersion are calculated and collected in Table 1. The efficiency $IE_w(\%)$ and surface coverage (θ) were determined by using the following Equations (9-10):

$$IE_w = \frac{W_{corr} - W'_{corr}}{W_{corr}} \times 100 \quad (9)$$

$$\theta = 1 - \frac{W'_{corr}}{W_{corr}} \Rightarrow \theta = \frac{(IE\%)}{100} \quad (10)$$

Where W_{corr} and W'_{corr} are the corrosion rates of the MS due to the dissolution in studied aggressive medium without and with the studied range of the EHDPTC concentrations, respectively, θ is the degree of surface coverage of the inhibitor. From the Table 1 and the Fig. 2, it is clear that increase of inhibitor concentration caused a decrease in the weight loss as well as corrosion rate of mild steel and, increasing the efficiency of inhibition to reach the maximum value of (IE_w=95.07%) at the highest concentration of 5×10^{-3} M. This shows that the molecule of EHDPTC may be adsorbed on the metal surface to cover the active sites on the electrode surface.

Table 1. Weight loss data of carbon steel in 1.0 M HCl for various concentrations of the EHDPTC at 303 K

Inhibitor	Concentration (M)	W_{corr}(mg cm^{-2} h^{-1})	η_w(%)	Ɵ
Blank	0	1.135	-	-
EHDPTC	5×10^{-3}	0.056	95.07	0.9507
	1×10^{-3}	0.112	90.13	0.9013
	5×10^{-4}	0.211	81.45	0.8145
	1×10^{-4}	0.349	69.19	0.6919

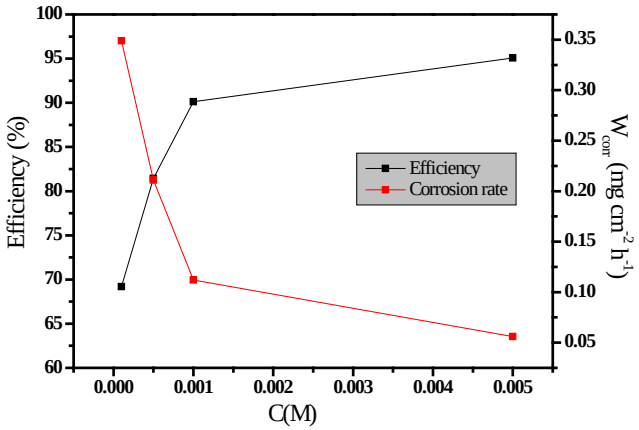

Fig. 2. Variation of inhibition efficiency and corrosion rate in 1.0 M HCl on carbon steel surface without and with different concentrations of EHDPTC

3.2. Potentiodynamic polarization curves

Typical polarisation potentiodynamic plots for carbon steel in 1.0 M HCl medium and in the presence of EHDPTC at 303 K are graphically presented in Fig. 3. Table 2 collected the parameters derived from *PDP* plots, while the values of efficiency IE_{Icorr} (%) are calculated using Equation 11.

$$IE_{Icorr} = \frac{I_{corr} - I'_{corr}}{I_{corr}} \times 100 \qquad (11)$$

Where I_{corr} and I'_{corr} are the corrosion current densities in uninhibited and inhibited medium, respectively.

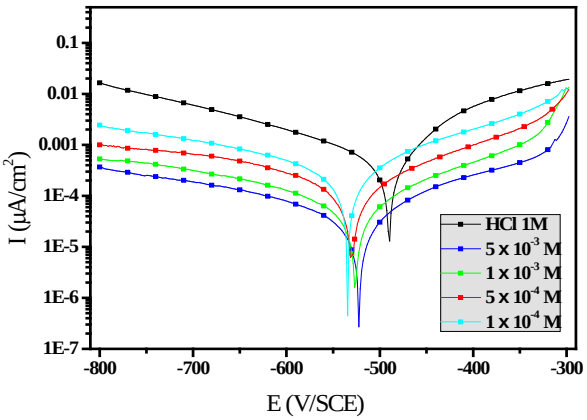

Fig. 3. Polarization curves of carbon steel in 1.0 M HCl for various concentrations of EHDPTC at 303 K

Table 2. Polarization data of carbon steel in 1.0 M HCl without and with various concentrations of EHDPTC at 303 K

Inhibitor	Concentration (M)	$-E_{corr}$ (mV/SCE)	$-\beta c$ (mV dec^{-1})	βa (mV dec^{-1})	I_{corr} (μA cm^{-2})	η_{Tafel} (%)
Blank	0	496.0	162	113.7	564.0	-
EHDPTC	5×10^{-3}	525.0	154	98.5	38.8	93.12
	1×10^{-3}	528.8	169	101.3	84.2	85.07
	5×10^{-4}	532.6	176	99.8	116.6	79.32
	1×10^{-4}	537.1	167	103.1	162.6	71.17

Analysis of the PDP curves indicates that the addition of EHDPTC decreases both cathodic and anodic current densities with the rise in the EHDPTC concentration. The presence of tested inhibitor in the aggressive medium causes change in the anodic and cathodic branches with no significant trend in the shift of E_{corr}values in all tested concentrations, suggesting that the EHDPTC, in general, behaves as mixed type inhibitor with no change in the corrosion mechanism occurred due to the addition of the inhibitor. Same behavior of the inhibitor was found by Larouj et al. during the study of the effect of 3-hydroxy-4, 6-dioxo pyrimido [2,1b][1,3] thiazine-7-carbonitrile derivatives[23]. By inspecting the results in Table 2, we note that the I_{corr} decreases monotonically when the content of EHDPTC increases in solution. The current density I_{corr} reaches a value of 38.8 μA/cm^2 at t concentration of 5×10^{-3} M of the inhibitor. This value of I_{corr} led to an *IE*% of about 93.12% and confirm that the EHDPTC is a good inhibitor against the corrosion of carbon steel in HCl medium. The values of the cathodic $\beta_{c,}$ show slight changes with the presence of EHDPTC, these results suggests that the surface blocking effect of the adsorbed EHDPTC diminish the anodic and cathodic reactions[24].

3.3. Electrochemical Impedance Spectroscopy Measurements *EIS*

The efficiency of EHDPTC on the carbon steel corrosion in the hydrochloric acidic medium (1.0 M HCl) was performed by means of EIS method at 303 K after 30 min of immersion. Fig. 4 represents the influence of EHDPTC concentrations on Nyquist impedance spectra. In the EIS experiments, with presence and absence of EHDPTC, only single semicircles are observed with depression at low frequency. This depression is often associated to the non-homogeneity and roughness of the MS surface [25]. A remarkable increase of the depressed semicircle diameter is observed with the presence of EHDPTC. generally, the EIS plots, loop-like capacitive is mainly attributed to the charge transfer process, while the increase of semicircle diameter with a rise in EHDPTC concentration is the result of the adsorption of the inhibitor on the carbon steel surface [26].

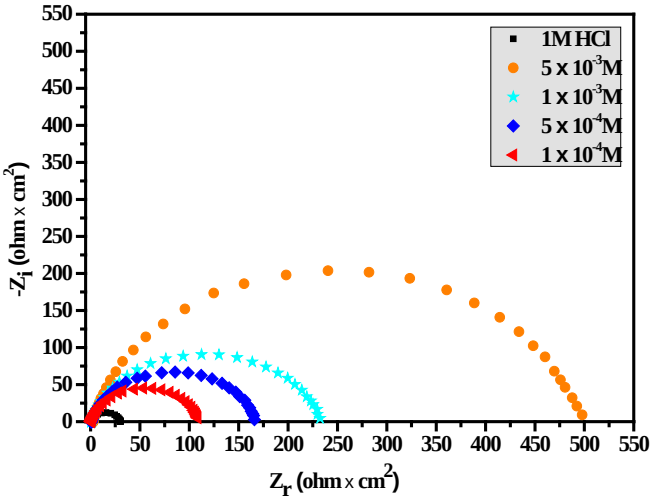

Fig. 4. Nyquist diagrams for carbon steel in 1.0 M HCl containing different concentrations of EHDPTC at 303 K

The equivalent circuit model is shown in Fig. 5 was used to analyse the *EIS* experiments, the parameters are collected in Table 3, while the double layer capacitance (C_{dl}) values are calculated using the Equation (12):

$$C_{dl} = \sqrt[n]{\mathrm{Q}.\mathrm{R_{ct}}^{1-\mathrm{n}}} \qquad (12)$$

where Q is the *CPE* constant and n is a coefficient that can be used as a measure of surface inhomogeneity [27]. The Equation (13) was used to calculate the IE_{Rct}%:

$$IE_{Rct} = \frac{R_{ct} - R'_{ct}}{R_{ct}} x100 \qquad (13)$$

Where R_{ct} and R'_{ct} are the charge transfer resistance values in with and without EHDPTC, respectively.

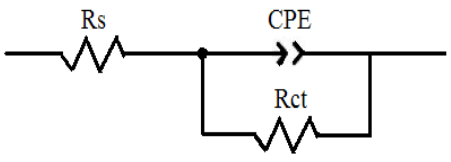

Fig. 5. The electrochemical equivalent circuit used to fit the impedance spectra.

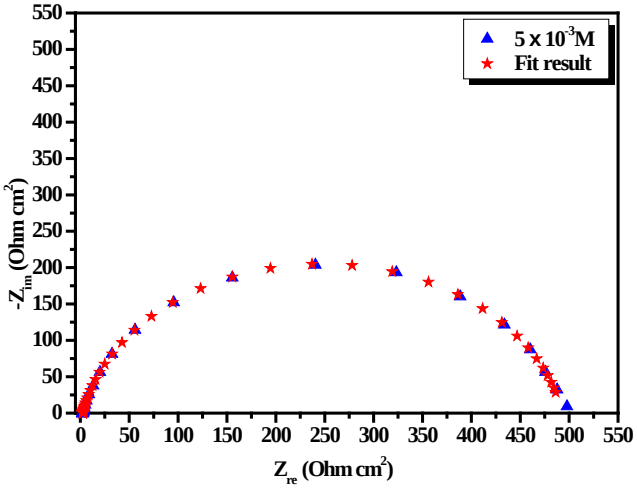

Fig. 6. Curve fitting of EIS data of carbon steel in 1.0 M HCl with 5×10^{-3} M of EHDPTC to Nyquist plots at E_{corr}

Table 3. Impedance parameters for corrosion of carbon steel in 1.0 M HCl in the absence and presence of different concentrations of EHDPTC at 303 K

Inhibitor	**Concentration (M)**	**R_{ct} (Ω cm^2)**	**n**	**$Q\times10^{-4}$ ($s^n\ \Omega^{-1}cm^{-2}$)**	**C_{dl} (μF cm^{-2})**	**η_z (%)**
Blank	0	29 .35	0.91	1.7610	97.23	-
EHDPTC	5×10^{-3}	490.8	0.90	0.2276	13.81	94.02
	1×10^{-3}	231.7	0.90	0.3265	18.97	87.33
	5×10^{-4}	166.9	0.89	0.4553	24.91	82.41
	1×10^{-4}	109.0	0.91	0.6414	39.26	73.08

In the presence of the EHDPTC, a high increase is observed in the values ofR_{ct}, while the C_{dl} values (Table 3) follow the opposite trend. The increase of the R_{ct} and the decrease in C_{dl} values demonstrate that the EHDPTC adsorbed in the carbon steel surface by the formation of an insulating protective film [28]. The *IE*% values obtained in the EIS study were in good correlation with those calculated in PDP studies.

It's reported that the inhibitors can adsorb through the lone pairs of electrons and π-bonds presented in their nitrogen, oxygen and sulfur atoms and aromatic rings, respectively [29], which may be the origin of the effectiveness in the present study.

3.4. Effect of temperature and thermodynamic activation parameters

Temperature has a great effect on the rate of metal electrochemical corrosion. In case of corrosion in an acid medium, the corrosion rate increases exponentially with temperature

increase because the hydrogen evolution over potential decreases [30]. Typical polarisation potentiodynamic plots for MS in 1.0 M HCl medium and in the presence of EHDPTC at temperature ranging from 303 to 333 K are graphically presented in Fig. 7a-b. Table 4 collected the parameters derived from PDP plots. The results reported in Table 4 showed that the I_{corr} values decrease with the increasing temperature in the absence and the presence of EHDPTC.

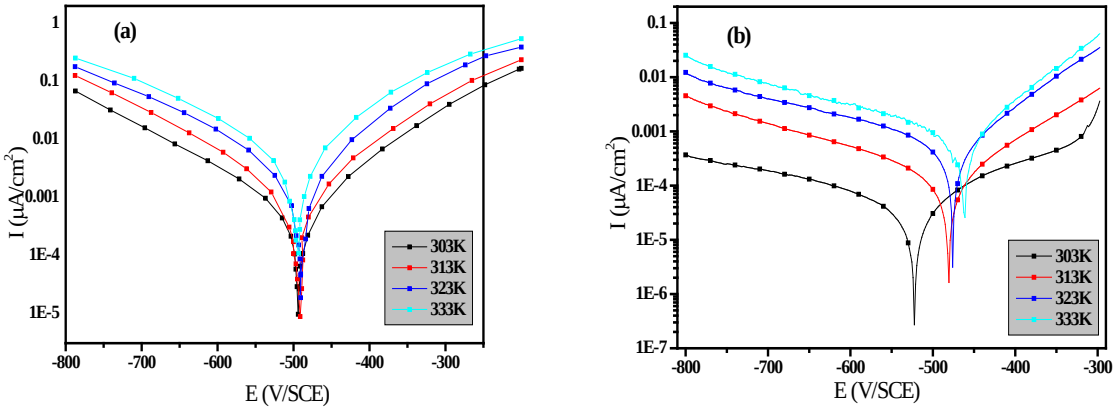

Fig. 7. Potentiodynamic polarization curves of carbon steel in 1.0 M HCl (a) and in the presence of 5×10^{-3} M EHDPTC; (b) at different temperatures

Table 4. The influence of temperature on the electrochemical parameters for carbon steel electrode immersed in 1.0 M HCl and 1.0 M HCl+5×10^{-3} M EHDPTC

Inhibitor	**Temperature (K)**	**$-E_{corr}$ (mV/SCE)**	**$-\beta c$ (mV dec^{-1})**	**βa (mV dec^{-1})**	**I_{corr} (μA cm^{-2})**	**η_{Tafel} (%)**
Blank	303	496	162.5	113.7	564	-
	313	498	154.5	101.4	773	-
	323	492	176.0	98.4	1244	-
	333	497	192.0	110.1	1650	-
EHDPTC	303	525	154	116.8	38.8	93.12
	313	483	144.7	103.9	106.1	86.27
	323	480	149.9	104.5	332.0	73.31
	333	465	179.8	107.9	652.9	60.43

The activation parameters for the corrosion process were calculated from Arrhenius type plot according to the following equations:

$$I_{corr} = A\ exp\left(\frac{-E_a^*}{RT}\right) \quad (14)$$

$$I_{corr} = \frac{RT}{Nh}\, exp\left(\frac{\Delta H_a^*}{R}\right) exp\left(-\frac{\Delta S_a^*}{RT}\right) \quad (15)$$

Where I_{corr} is corrosion current density, k is the Arrhenius pre exponential factor, R is the gas constant, h is the Planck's constant and N is Avogadro's number. According to the data in Table 5, the plots of ln(I_{corr}) versus 1/T (Figure 8a) and ln(I_{corr} /T) versus 1/T (Figure 8b) show almost straight lines and all the regression coefficients are close to 1. From the slopes and intercepts of the straight lines, the values of E_a^*, ΔH_a^* and ΔS_a^* were calculated and listed in Table 5.

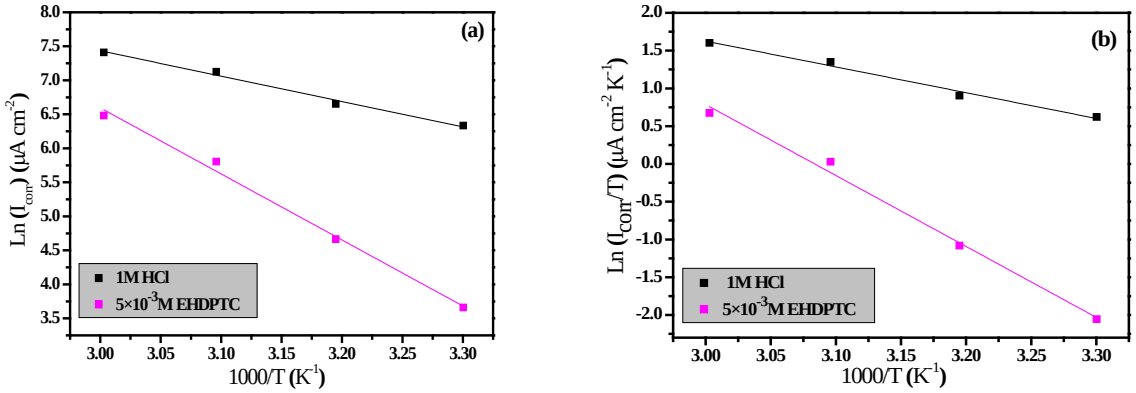

Fig. 8. Arrhenius plots (a) and Transition state plots(b) for carbon steel in 1.0 M HCl and 1.0 M HCl+5×10^{-3} M EHDPTC

Table 5. Corrosion kinetic parameters for carbon steel in 1.0 M HCl in the absence and presence of 5×10^{-3} M EHDPTC

Inhibitor	**E_a^* (kJ/mol)**	**ΔH_a^* (kJ/mol)**	**ΔS_a^* (J mol-1 K^{-1})**	**$E_a^* - \Delta H_a^*$**
1 M HCl	31.00	28.35	-98.8	2.65
5×10^{-3} EHDPTC	80.74	78.09	43.28	2.65

It was clear that the values of E_a^* in the presence of the EHDPTC are higher than those in the uninhibited acid solution. These results are in accord with the reported studies [23,24]. The increase in the apparent activation energy E_a^* at low inhibitor concentrations, at pH=1 (Table 5), may be interpreted as physical adsorption that occurs in the first stage [31,32].

Examination of data obtained in Table 5, reveals that the values of ΔH_a^* and ΔS_a^* in the presence of the additives increase over that of the uninhibited solution. This implies that energy barrier of the corrosion reaction in the presence of EHDPTC increases which is expected. The positive values of ΔH_a^* show the endothermic nature of the dissolution process.

The large negative value of ΔS_a^* for carbon steel in 1.0 M HCl implies that the activated complex is the rate-determining step, rather than the dissociation step. In the presence of the inhibitor, the value of ΔS_a^* increases and is generally interpreted as an increase in disorder as the reactants are converted to the activated complexes [33]. The positive values of ΔS_a^* reflect the fact that the adsorption process is accompanied by an increase in entropy, which is the driving force for the adsorption of the inhibitor onto the steel surface.

3.5. Adsorption isotherm and thermodynamic adsorption parameters

On the basis of evaluation of the interaction between the inhibitor and steel surface, it is important to consider the adsorption isotherms to analyze the mechanism and nature of the adsorption processes of chemicals species on the carbon steel surface [34]. Attempts were made to fit θ values to various isotherms including Langmuir, Frumkin, Temkin and Flory–Huggins isotherms as follows [35,36]:

$$\frac{C}{\theta} = \frac{1}{K_{ads}} + C \quad (16)$$

$$\exp(f\theta) = K_{ads}\, C \quad (17)$$

$$\frac{\theta}{(1-\theta)}\exp(-f\theta) = K_{ads}\, C \quad (18)$$

$$\log(\theta/C) = \log(K_{ads}) + a \times (1-\theta) \quad (19)$$

θ is the surface coverage, K_{ads} is the adsorption–desorption equilibrium constant, C is the concentration of inhibitor and *f* is the factor of energetic inhomogeneity. Again, the weight loss measurements were employed in this experiment with the concentration range 5×10^{-3}–1×10^{-4} M at 303 K.

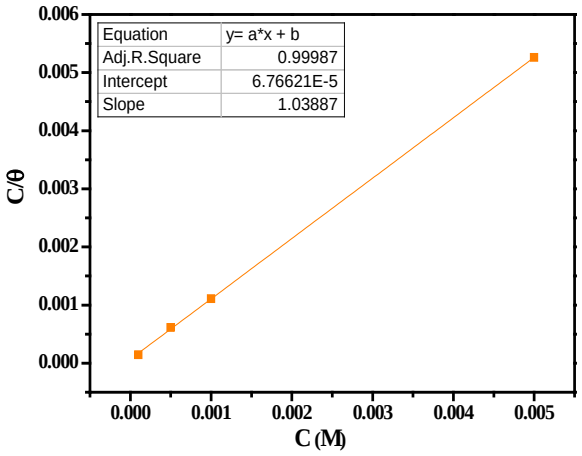

Fig. 9. Langmuir adsorption of EHDPTC on the carbon steel surface in 1.0 M HCl solution at 303 K

The Langmuir model was found to be the best fit among various tested isotherms (Frumkin, Temkin and Flory–Huggins) and consequently the good descriptor for adsorption of the EHDPTC on the carbon steel surface (Fig .8) [37].

$$\frac{C_{inh}}{\theta} = \frac{1}{K_{ads}} + C_{inh} \quad (20)$$

Where K_{ads} is the equilibrium constant of the adsorption process, C_{inh} is the concentration of the tested compound in the solution. The free energy of adsorption ΔG_{ads} was calculated using the values of $K_{ads}$by the Equation [37]:

$$\Delta G_{ads} = -RTln(K_{ads} * C_{solvent}) \quad (21)$$

Where: $C_{solvent}$ is the molar concentration of solvent (For H_2O is 55.5 mol L^{-1}).

Table 6. The adsorption parameters for the corrosion of carbon steel in 1.0 M HCl at 303K

Inhibitor	**Slope**	**K_{ads} (M^{-1})**	**R^2**	**ΔG_{ads}(kJ/mol)**
EHDPTC	1.03	34022.5	0.99987	- 34.31

The largeK_{ads} value (Table 6) obtained in this study; indicates the strong interaction between the carbon steel surface and adsorbing molecules of EHDPTC, which support the better-obtained IE % [38].

Optimized Geometry HOMO LUMO

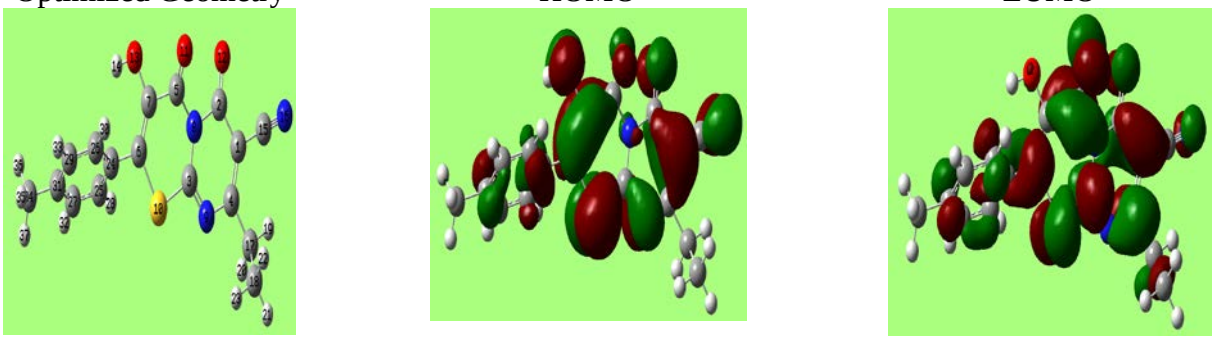

Fig. 10. Optimized molecular structure and frontiers orbitals distribution HOMO and LUMO of the inhibitor EHDPTC

While the negative values of the adsorption free energy ΔG_{ads} suggest that the EHDPTC molecule adsorb spontaneously onto the carbon steel surface and the protective film is highly stable [38]. The calculated value of ΔG_{ads} is around - 34.31 kJ/mol, which may indicate that the adsorption mechanism of EHDPTC on carbon steel is complex mixed type adsorption,

neither typical chemisorption nor typical physisorption, but involving both interactions types with a remarkable predominance of chemical interactions [39].

3.6. Quantum chemical calculation

3.6.1. Individual reactivity parameters

The optimized geometry and the highest occupied molecular orbital (HOMO) and the lowest unoccupied molecular orbital (LUMO) densities of the neutral specie of the studied compound by B3LYP-6-31G (d, p) are shown in Fig. 10.

In EHDPTC, it is seen from the HOMO and LUMO that the electron density is distributed over the entire molecule. It can be concluded from these observations that these atoms (S(10),N(8) and N(9)) and groups (C=O, C≡N and O-H) are mainly responsible for the interaction with metal surfaces.

Previous studies[40–42] have shown that quantum chemical parameters such as the energy of the HOMO (E_{HOMO}), energy of the LUMO (E_{LUMO}), dipole moment, etc., can be utilized to understand the adsorption phenomenon of the inhibitor on the metal surface. Table 7 reports the quantum chemical parameters investigated in this work.

Table 7. Calculated quantum chemical parameters of the inhibitor molecule

Quantum Parameters	**μ Debye**	**TE (a.u)**	**E_{HOMO} (eV)**	**E_{LUMO} (eV)**	**ΔE_{L-H} (eV)**	**I (eV)**	**A (eV)**	**η (eV)**	**σ (eV^1)**	**χ (eV)**	**ΔN (eV)**
EHDPTC	11.9	1443	-6.342	-2.427	3.915	6.342	2.427	1.957	0.511	4.38	0.11

The value of E_{HOMO} is likely to indicate a tendency of inhibitor molecule to donate electron to appropriate acceptor molecules with low energy or empty electron orbital. The value of E_{LUMO}, indicates the tendency of inhibitor molecule to accept electrons [43]. The transfer of electron from inhibitor molecule to the metallic surface will occur when $\Delta N>0$ and vice versa when $\Delta N<0$ [44–46]. Elnga *et al.* have reported that there is an increase in electron donation capability of inhibitor molecules when the ΔN value is less than 3.6[47]. From Table 7, it is observed that the calculated $\Delta N=0.11$ eV is positive and lower than 3.6, which strongly indicates that the inhibitor has the capability in donating electrons to the vacant d-orbital of metal.

3.6.2. Actives sites and Selectivity parameters: the $f^{\pm}$Fukui function

To investigate reactive sites in the tested inhibitor, electrostatic surface potential (ESP) maps provide a visual method to understand the region of the electrophilic attack, nucleophilic attack and the electrostatic potential zero regions [48]. The total electron density

surface mapped with molecular electrostatic potential (MEP) of EHDPTC is shown in Fig.11. In these maps, the different values of the electrostatic potential were demonstrated with the help of different colors which are red, yellow, green, light blue and blue. The red and yellow colors suitable for the negative parts of the MEP are linked to electrophilic reactivity, blue colors suitable for the positive parts to the nucleophilic reactivity and the green color represents the electrostatic potential zero region. As can be seen in Fig. 11 that the red and yellow sites are mainly observed over the functional groups (O-H, C=O and C≡N) and the conjugated double bonds, the green regions are mainly localized around the heteroatoms (S10, N8, N8) and the ethyl group. The blue and light blue regions are mainly localized around the benzene ring substituted by the methyl group. These remarks confirmed by the mulliken charges of the atoms as can be seen from the Fig.11 [49]. As noticed that the carbon steel acting as an electrophilic, and the nucleophilic centers are heteroatoms with free electron pairs and π-electrons in conjugated double bonds. The inhibitor can promote formation of a chelate on the carbon steel surface by transferring electrons from inhibitor molecules to iron atom d-orbital and forming a coordinate covalent bond through the chemical adsorption[50].

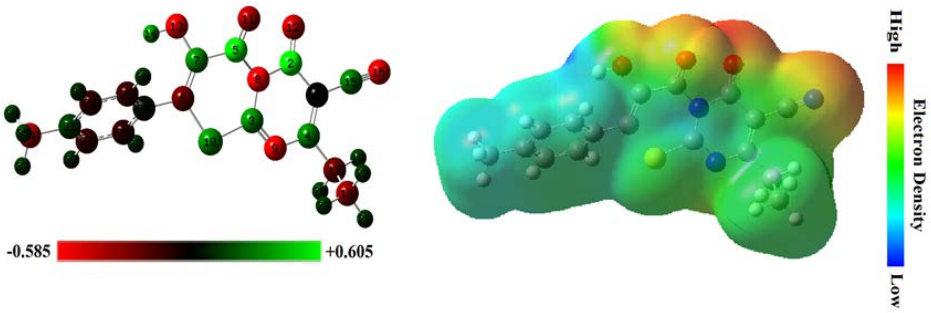

Fig. 11. Electrostatic properties of EHDPTC, side view of the Mulliken charge populations is displayed on the left while and right panels show the isosurface representation of electrostatic potential respectively

In order to obtain additional information about the donor-acceptor interactions, the Fukui function (FF) calculations are one of the useful means for this purpose. The local reactivity indices also define the most reactive regions in a molecule. The nucleophilic and electrophilic behaviour of different sites of the inhibitor molecule are mainly determined by the maximum threshold f_k^+ and f_k^- values. When a molecule accepts electrons the changes in electron density are measured by the f_k^+values while the f_k^- values give the measures of the changes in electron density when the electrons are lost by the molecules. The high f_k^+ and f_k^- values imply the high electron acceptance and donation capabilities of the molecules, respectively. From the calculated Fukui indices (Table 8); it can be observed that the most susceptible sites for electron acceptance or donation are the N, O, S heteroatoms, followed by some C atoms

of the heterocycle rings. For EHDPTC, the favorable centers for electron acceptance *i.e.*, nucleophilic attacks are C(1), C(6), C(7), N(9), N(10), O(12) and O(13) atoms having f_k^+ values -0.10288, -0.07747, -0.08369, -0.16544, -0.07484, -0.08035 and -0.11678 respectively. On the other hand, the susceptible sites for electrophilic attacks *i.e.*, electron donation are C(4), C(5), C(6), S(10), O(11) and N(16) atoms having f_k^- values -0.08439, -0.09251, -0.08093, -0.10689, -0.09928 and-0.09689 respectively. Furthermore, it is seen from the Fukui function f_k^+ and f_k^- values that, S atom in the EHDPTC molecules have tremendous electron donation and acceptance capability and perhaps it creates the major differences in their higher binding abilities.

Table 8. Natural population and Fukui functions of EHDPTC, calculated at B3LYP/6- 31G (d, p) in gas phase

Atom	$P_k(N)$	$P_k(N-1)$	$P_k(N+1)$	f_k^+	f_k^-
C 1	6.30609	6.35954	6.20321	-0.10288	-0.05345
C 2	5.30932	5.32229	5.31564	0.00632	-0.01297
C 3	5.69793	5.74189	5.71441	0.01648	-0.04396
C 4	5.69831	5.78270	5.69368	-0.00463	-0.08439
C 5	5.33113	5.42364	5.34286	0.01173	-0.09251
C 6	6.26263	6.34356	6.22324	-0.03939	-0.08093
C 7	5.76245	5.73874	5.68498	-0.07747	0.02371
N 8	7.51479	7.50590	7.51054	-0.00425	0.00889
N 9	7.53568	7.55208	7.45199	-0.08369	-0.0164
S 10	15.52988	15.63677	15.36444	-0.16544	-0.10689
O 11	8.47101	8.57029	8.41619	-0.05482	-0.09928
O 12	8.5248	8.57601	8.44996	-0.07484	-0.05121
O 13	8.66478	8.67634	8.58443	-0.08035	-0.01156
C 15	5.72099	5.70171	5.74242	0.02143	0.01928
N 16	7.29661	7.39350	7.17983	-0.11678	-0.09689
C 17	6.49864	6.48675	6.50762	0.00898	0.01189
C 18	6.68106	6.67506	6.68455	0.00349	0.006
C 24	6.11129	6.09551	6.12479	0.0135	0.01578
C 25	6.20581	6.22875	6.19203	-0.01378	-0.02294
C 26	6.23651	6.27860	6.22985	-0.00666	-0.04209
C 27	6.22103	6.23494	6.20863	-0.0124	-0.01391
C 29	6.22299	6.22879	6.20579	-0.0172	-0.0058
C 31	6.01098	6.07138	5.95759	-0.05339	-0.0604
C 34	6.70462	6.69063	6.71771	0.01309	0.01399

4. CONCLUSION

The corrosion inhibition of carbon steel in 1.0 M HCl solution by new pyrimidothiazine derivative was investigated using weight loss, electrochemical techniques and theoretical studies. According to experimental findings, the EHDPTC compound is good corrosion inhibitor for carbon steel in 1.0 M HCl solution and its performance depends on its concentration and its molecular structure. PDP measurements indicate that the EHDPTC acts as a mixed type inhibitor. EIS measurements also indicate that the inhibitor addition increases the charge transfer resistance and show that the inhibitive performance depends on molecules adsorption on metallic surface. The thermodynamic parameters of activation and adsorption are calculated and discussed. The high inhibition efficiency of the inhibitor was explained by adsorption of EHDPTC derivative molecule on carbon steel surface. Quantum chemical approach was adequately used to identify the most reactive centers in the tested compound.

REFERENCES

[1] K. Emregül, and M. Hayvalı. Mater. Chem. Phys. 83 (2004) 209.
[2] A. Döner, E. A. Şahin, G. Kardaş, and O. Serindağ. Corros. Sci. 66 (2013) 278.
[3] R. Solmaz. Corros. Sci. 52 (2010) 3321.
[4] R. Solmaz. Corros. Sci. 81 (2014) 75.
[5] G. Gece, and S. Bilgiç. Corros. Sci. 52 (2010) 3304.
[6] J. Radilla, G. E. Negrón-Silva, M. Palomar-Pardavé, M. Romero-Romo, and M. Galván. Electrochim. Acta. 112 (2013) 577.
[7] T. Arslan, F. Kandemirli, E. E. Ebenso, I. Love, and H. Alemu. Corros. Sci. 51 (2009) 35.
[8] H. Serrar, S. Boukhris, A. Hassikou, and A. Souizi, J. Heterocycl. Chem. 52 (2015) 1269.
[9] M. J. Frisch, G. Trucks, H. Schlegel, G. Scuseria, M. Robb, J. Cheeseman, G. Scalmani, V. Barone, B. Mennucci, G. Petersson, Gaussian 09, revision A. 1, Gaussian Inc Wallingford CT. (2009).
[10] R. Dennington, T. Keith, J. Millam, GaussView, version 5, Semichem Inc Shawnee Mission KS (2009).
[11] A. D. Becke. J. Chem. Phys. 98 (1993) 5648.
[12] C. Lee, W. Yang, R.G. Parr. Phys. Rev. B 37 (1988) 785.
[13] M. J. Dewar, and W. Thiel. J. Am. Chem. Soc. 99 (1977) 4899.
[14] R. G. Pearson. Chem. Inorg. Chem. 27 (1988) 734.
[15] P. Senet. Chem. Phys. Lett. 275 (1997) 527.
[16] V. Sastri, and J. Perumareddi. Corrosion 53 (1997) 617.
[17] I. Lukovits, E. Kalman, and F. Zucchi. Corrosion. 57 (2001) 3.

[18] M. Lebrini, F. Bentiss, N. E. Chihib, C. Jama, J. P. Hornez, and M. Lagrenée. Corros. Sci. 50 (2008) 2914.
[19] Z. Cao, Y. Tang, H. Cang, J. Xu, G. Lu, and W. Jing. Corros. Sci. 83 (2014) 292.
[20] A. Kokalj. Chem. Phys. 393 (2012) 1.
[21] R. G. Parr, and W. Yang. J. Am. Chem. Soc. 106 (1984) 4049.
[22] R. R. Contreras, P. Fuentealba, M. Galván, and P. Pérez. Chem. Phys. Lett. 304 (1999) 405.
[23] M. Larouj, M. Belkhaouda, H. Lgaz, R. Salghi, S. Jodeh, S. Samhan, H. Serrar, S. Boukhris, M. Zougagh, and H. Oudda. Der Pharma Chem. 8 (2016) 114.
[24] M. Larouj, M. Belayachi, H. Zarrok, A. Zarrouk, A. Guenbour, M.E. Touhami, A. Shaim, S. Boukhriss, H. Oudda, and B. Hammouti. Der Pharma Chem. 6 (2014) 373.
[25] K. Krishnaveni, J. Ravichandran. J. Electroanal. Chem. 735 (2014) 24.
[26] M. Yadav, D. Behera, and S. Kumar. Surf. Interface Anal. 46 (2014) 640.
[27] W. Chen, S. Hong, B. Xiang, H. Luo, M. Li, and N. Li. Corros. Eng. Sci. Technol. 48 (2013) 98.
[28] M. Chellouli, D. Chebabe, A. Dermaj, H. Erramli, N. Bettach, N. Hajjaji, M. Casaletto, C. Cirrincione, A. Privitera, and A. Srhiri. Electrochim. Acta. 204 (2016) 50.
[29] S. K. Saha, M. Murmu, N. C. Murmu, and P. Banerjee. J. Mol. Liq. 224 (2016) 629.
[30] A. Popova, E. Sokolova, S. Raicheva, and M. Christov. Corros. Sci. 45 (2003) 33.
[31] T. Szauer, and A. Brandt. Electrochim. Acta. 26 (1981) 1253.
[32] E. F. El Sherbini. Mater. Chem. Phys. 60 (1999) 286.
[33] M. Stern, and A. L. Geary. J. Electrochem. Soc. 104 (1957) 56.
[34] G. Avci. Mater. Chem. Phys. 112 (2008) 234.
[35] H. Lgaz, R. Salghi, S. Jodeh, Y. Ramli, M. Larouj, K. Toumiat, M. Quraishi, H. Oudda, and W. Jodeh. J. Steel. Struct. Constr. 2 (2016) 2472.
[36] A. Aouniti, H. Elmsellem, S. Tighadouini, M. Elazzouzi, S. Radi, A. Chetouani, B. Hammouti, A. Zarrouk. and J. Taibah, Univ. Sci. (2015).
[37] H. Lgaz, O. Benali, R. Salghi, S. Jodeh, M. Larouj, O. Hamed, M. Messali, S. Samhan, M. Zougagh, and H. Oudda. Pharma Chem. 8 (2016) 172.
[38] N. Soltani, M. Behpour, E. Oguzie, M. Mahluji, and M. Ghasemzadeh. RSC Adv. 5 (2015) 11145.
[39] A. Singh, S. Mohapatra, and B. Pani. J. Ind. Eng. Chem. 33 (2016) 288.
[40] M. M. Kabanda, S. K. Shukla, A. K. Singh, L. C. Murulana, and E. E. Ebenso. Int. J. Electrochem. Sci. 7 (2012) 8813.
[41] M. M. Kabanda, L. C. Murulana, and E. E. Ebenso. Int. J. Electrochem. Sci. 7 (2012) 7179.
[42] M. M. Kabanda, and E. E. Ebenso. Int. J. Electrochem. Sci. 7 (2012) 8713.
[43] G. Gece. Corros. Sci. 50 (2008) 2981.

[44] S. K. Saha, A. Dutta, P. Ghosh, D. Sukul, and P. Banerjee. Phys. Chem. Chem. Phys. 17 (2015) 5679.
[45] S. K. Saha, and P. Banerjee. RSC Adv. 5 (2015) 71120.
[46] Z. Cao, Y. Tang, H. Cang, J. Xu, G. Lu, and W. Jing. Corros. Sci. 83 (2014) 292.
[47] M. K. Awad, M. R. Mustafa, and M. M. A. Elnga. J. Mol. Struct. Theochem. 959 (2010) 66.
[48] N. Okulik, and A. H. Jubert. Internet. Electron. J. Mol. Des. 4 (2005) 17.
[49] H. Tian, W. Li, K. Cao, and B. Hou. Corros. Sci. 73 (2013) 281.
[50] P. Fuentealba, P. Pérez, and R. Contreras. J. Chem. Phys. 113 (2000) 2544.